Inorg. Chem. **2004**, *43*, 5543–5549

Synthesis and Photochemical Properties of a Novel Iron–Sulfur–Nitrosyl Cluster Derivatized with the Pendant Chromophore Protoporphyrin IX[1]

Christa L. Conrado,[†] Stephen Wecksler,[†] Christian Egler,[†,2] Douglas Magde,[‡] and Peter C. Ford*,[†]

Department of Chemistry & Biochemistry, University of California, Santa Barbara, California 93106-9510, and Department of Chemistry & Biochemistry, University of California, San Diego, California 92093-0332

Received April 27, 2004

The novel Roussin red-salt ester (**PPIX-RSE**) with a pendant porphyrin chromophore was prepared and investigated as a precursor for the photochemical generation of nitric oxide. **PPIX-RSE** has the general formula $Fe_2(NO)_4\{(\mu\text{-}S,\mu\text{-}S')P\}$ (where (S,S′)P is the bis(2-thiolatoethyl) diester of protoporphyrin IX. The photoexcitation of **PPIX-RSE** with 436- or 546-nm light in an aerated chloroform solution led to the photodecomposition of the cluster with the respective quantum yields $(5.2 \pm 0.7) \times 10^{-4}$ and $(2.5 \pm 0.5 \times 10^{-4})$ and the concomitant release of NO. **PPIX-RSE** is a significantly more effective NO generator at longer wavelength excitation than are other $Fe_2(\mu\text{-}SR)_2(NO)_4$ esters for which R is a simple alkyl group such as CH_3CH_2– because of the much higher absorptivity of the pendant **PPIX** chromophore at these wavelengths and a modestly higher quantum yield. Fluorescence intensity and lifetime data indicate that the photoexcited porphyrin of **PPIX-RSE** is largely quenched by the energy transfer to the $Fe_2S_2(NO)_4$ cluster's core. However, a small fraction of this emission is not quenched, and it is proposed that **PPIX-RSE** may exist in solution as two conformers.

Introduction

Nitric oxide (nitrogen monoxide) is well known to play important roles in mammalian biology as a bioregulatory molecule and as a toxic agent formed in immune response to pathogen invasion.[3] Furthermore, NO has also been shown to sensitize hypoxic cells to ionizing radiation,[4] and thus it may serve to enhance the cell-killing effect of γ-radiation in treating solid tumors. In these contexts, ongoing studies in this laboratory have been concerned with the photochemically activated delivery of NO to specific physiological targets on demand.[5] Earlier work here demonstrated that the iron–sulfur–nitrosyl cluster anions $Fe_4S_3(NO)_7^-$ ("Roussin's black salt" anion, **RBS**) and $Fe_2(\mu\text{-}S_2)(NO)_4^{2-}$ ("Roussin's red salt" dianion, **RRS**) release NO with moderate quantum yields upon photolysis.[6] It was shown that visible-light irradiation of V79 Chinese hamster cell cultures treated first with Roussin's red salt enhanced the cell-killing effectiveness of γ-radiation, and it was concluded that the NO released photochemically is the sensitizer responsible for this effect. However, **RRS** does not have the high optical absorptivity at longer wavelengths desirable for a photoreactive material to be used in mammalian tissues. This led to an interest in developing derivatives of **RRS** with substituents that incorporate chromophores having desirable spectra and other tunable properties.

* Author to whom correspondence should be addressed. E-mail: ford@chem.ucsb.edu.
† University of California, Santa Barbara.
‡ University of California, San Diego.

(1) Taken in part from the Ph.D. Dissertation of C. L. Conrado, University of California, Santa Barbara, 2002.
(2) Undergraduate student from Westfaelische Wilhelms-Universitaet, Muenster, Germany.
(3) (a) Ignarro, L. J., Ed. *Nitric Oxide: Biology and Pathobiology*; Academic Press: San Diego, CA, 2000. (b) Fang, F. C., Ed. *Nitric Oxide and Infection*; Kluwer Academic/Plenum Publishers: New York, 1999. (c) Wink, D. A.; Hanbauer, I.; Grisham, M. B.; Laval, F.; Nims, R. W.; Laval, J.; Cook, J.; Pacelli, R.; Liebmann, J.; Krishna, M.; Ford, P. C.; Mitchell, J. B. *Curr. Top. Cell. Regul.* **1996**, *34*, 159
(4) (a) Howard-Flanders, P. *Nature (London)* **1957**, *180*, 1191. (b) Russo, A.; Mitchell, J. B.; Dinkelstein, E.; DeGraff, W. G.; Spiro, I. J.; Gamson, J. *Radiat. Res.* **1985**, *103*, 232−239. (c) Mitchell , J. B.; Wink, D. A.; DeGraff, W.; Gamson, J.; Keefer, L. K.; Krishna, M. C. *Cancer Res.* **1993**, *53*, 5845. (d) Chung, P.; Cook, T.; Liu, K.; Vodovotz, Y.; Zamora, R.; Finkelstein, S.; Billiar, T.; Blumberg, D. *Nitric Oxide* **2003**, *8*, 119−126
(5) Ford, P. C.; Bourassa, J.; Miranda, K.; Lee, B.; Lorkovic, I.; Boggs, S.; Kudo, S. Laverman, L. *Coord. Chem. Rev.* **1998**, *171*, 185.
(6) (a) Bourassa, J.; DeGraff, W.; Kudo, S.; Wink, D. A.; Mitchell, J.; Ford, P. C. *J. Am. Chem. Soc.* **1997**, *119*, 2853. (b) Bourassa, J.; Ford, P. C. *Coord. Chem. Rev.* **2000**, *200*, 887−900.

10.1021/ic049459a CCC: $27.50
Published on Web 08/04/2004

Roussin's red salt esters (**RSE**), $Fe_2(\mu\text{-}SR)_2(NO)_4$, can be prepared from the reaction of **RRS** with an alkyl halide (eq 1).[7]

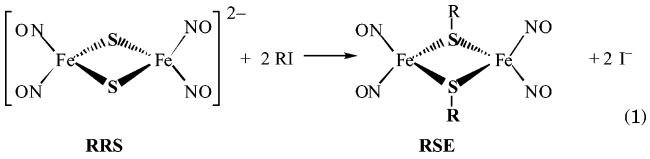

RRS **RSE** (1)

Continuous wave (CW) photolysis studies in this laboratory have demonstrated that **RSE** compounds release NO upon irradiation ($\lambda_{irr} = 365$ nm) in aerated solutions and that ~4 mol of NO is generated for each mole of **RSE** that undergoes photoconversion.[8,9] Thus, the **RSE** complexes would appear to be promising candidates for photochemical NO precursors; however, when R is a simple alkyl group, these compounds are only weak absorbers at the longer visible-range wavelengths. To address this issue, one can envision utilizing eq 1 to construct new esters where R− is a chromophore with a much larger absorptivity in the visible region. Described here are the synthesis and photochemical/physical properties of the supramolecular complex **PPIX-RSE** consisting of the **RSE** chromophore covalently linked to a red-absorbing antenna derived from protoporphyrin IX (**PPIX**), a strongly absorbing chromophore at longer wavelengths.[10] The photochemical properties of this species will be compared with those of related compounds. Additional interest in **PPIX** systems is derived from the possibility that porphyrin derivatives may have biological specificity in terms of localizing in certain tissues.[11]

Experimental Section

Materials. PPIX and its dimethyl ester **PPIX-DME** were purchased from Aldrich. The water for the spectroscopic studies was purified by a Millipore system. Methanol was distilled under nitrogen from I_2 and Mg. THF was distilled under N_2 over sodium and benzophenone. Chromatography-grade argon was used as received from Air Liquide. All inert-atmosphere manipulations were performed on a vacuum manifold. Deaeration of the solutions was achieved by three freeze−pump−thaw (f−p−t) cycles. Nitric oxide (99.0%) was purchased from Matheson and was passed through a stainless steel column filled with Ascarite II to remove higher nitrogen oxides. Stainless steel tubing and fittings were used, and manifold connections were stainless steel-to-glass fittings. Roussin's red ester compounds, $Fe_2(\mu\text{-}SCH_2CH_3)_2(NO)_4$ (**I**) and $Fe_2(\mu\text{-}SCH_2C_6H_5)_2(NO)_4$ (**II**), were prepared as described previously.[12] The red esters are moderately air- and light-sensitive and require storage in the dark under an inert atmosphere.

Instruments. UV−vis absorption spectra were recorded for solutions in 1-cm quartz cells using an HP8572 diode array spectrophotometer. Infrared spectra were obtained in an IR cell with CaF_2 windows using a BioRad FTS 60 SPC 3200 FTIR spectrometer. Solution NO was analyzed electrochemically with a Harvard Apparatus nitric oxide analyzer.

Emission Studies. Emission studies were carried out on a SPEX Fluorolog spectrofluorimeter. The samples were dissolved in chloroform or tetrahydrofuran under aerated conditions such that the absorbance values were approximately unity at the excitation wavelength of 404 nm. The emission spectra were fluorescence scanned from 420 to 750 nm. Deaerating the solutions had little effect on the emission spectra or intensities.

Fluorescence decays were characterized by time-correlated single-photon counting (TCSPC) at UC San Diego. A neodymium: vanadate laser at 530 nm (Coherent Verdi) pumped a custom-built titanium:sapphire laser that generated femtosecond mode-locked pulses by self-phase locking. Harmonic doubling provided excitation pulses near 400 nm. A portion of the beam was picked off and sent to a photodiode to provide "stop" pulses. Emission from solutions in ordinary luminescence cells was collected and sent through a half-meter monochromator (Spex 1870) to a microchannelplate photomultiplier (Hamamatsu 1564U-01). After amplification (Philips 774), the pulses were recognized by a constant-fraction discriminator (Tennelec TC454) to provide "start" signals to the time analyzer (Canberra 2044). The stop pulses came from the photodiode through a separate discriminator (EGG-Ortec 934). On this occasion, pulse selection was not used. Electronic gating[13] was employed to avoid a data pile-up at the time analyzer. The histogram of the delay times between fluorescence and excitation was collected by a multichannel pulse-height analyzer (Norland 5300) and transferred to a microcomputer for processing. The instrument response function to instantaneous emission was measured using a colloidal suspension. Deconvolution was carried out using iterative reconvolution within a least-squares routine based on the Marquardt method[14] with an in-house program incorporating insights from Grinvald and Steinberg.[15] It also accommodates an infinite sequence of excitation pulses producing decays longer than the repetition period. For exponential decays, this involves summing a simple geometric series for each fit component. A general introduction to the methodology was provided previously;[16] however, the internal reference described in that report was not used with the current laser system.

Photochemical Experiments. Continuous-wave photolysis studies were performed using an optical train with a 200-W Hg arc lamp as the light source. Interference filters were used to isolate appropriate excitation wavelengths. Light intensities were determined using ferric oxalate or Reinecke's salt (>436 nm) as chemical actinometers. All solutions were stirred continuously and protected from extraneous light. Known concentrations of the samples were prepared and irradiated under aerated conditions. The light intensity for the photolysis experiments ranged from 1.0×10^{-6} to 3.0×10^{-6} Ein L^{-1} s^{-1}.

(7) (a) Complexes of the structure $Fe_2(SR)_2(NO)_4$ have been described as esters in earlier literature. (b) Butler, A. R.; Glidewell, C.; Hyde, A. R.; McGinnis, J.; Seymore, J. S. *Polyhedron* **1993**, *2*, 1045−1052. (b) Butler, A. R.; Glidewell, C.; Johnson, I. L. *Polyhedron* **1987**, *6*, 2091−2094. (c) Glidewell, C.; Lambert, R. J. *J. Chem. Soc., Dalton Tans*. **1990**, 2685−2690.

(8) Conrado, C. L.; Bourassa, J. L.; Egler, C.; Wecksler, S.; Ford, P. C. *Inorg. Chem*. **2003**, *42*, 2288−2293.

(9) Bourassa, J. L. Photochemical Studies of Iron−Sulfur-Nitrosyls: Roussin's Salts and Related Compounds. Ph.D. Dissertation, University of California, Santa Barbara, CA, 1998.

(10) **PPIX** = 7,12-diethenyl-3,8,13,17-tetramethyl-2,18-porphine-dipropionic acid.

(11) (a) Anreoni, A., Cubeddu, R., Eds. *Porphyrins in Tumor Therapy*; Plenum Press: New York, 1984. (b) Phillips, D. *Pure Appl. Chem*. **1995**, *67*, 117−126.

(12) (a) Seyferth, D.; Gallagher, M. K.; Cowie, M. *Organometallics* **1986**, *5*, 539−548. (b) Glidewell, C.; Lambert, R. J.; Harman, M. E.; Hursthouse, M. B. *J. Chem. Soc., Dalton Trans*. **1990**, 2685−2690.

(13) Laws, W. R.; Potter, D. W.; Sutherland, J. C. *Rev. Sci. Instrum.* **1984**, *55*, 1564

(14) Marquardt, D. W. *J. Soc. Ind. Appl. Math.* **1963**, *11*, 431−441.

(15) Grinvald, A.; Steinberg, I. Z. *Anal. Biochem.* **1974**, *59*, 583−598.

(16) Magde, D.; Campbell, B. F. *SPIE Proceedings* **1989**, *1054*, 61−68.

Syntheses. Protoporphyrin IX Bis-(2-iodoethyl) diester) (PPIX-I). A round-bottom flask equipped with a stir bar was charged with protoporphyrin IX (0.5643 g; 1.00 mmol) and ∼50 mL of dry, distilled THF. After dissolution, 1-hydroxybenzotriazole (0.271 g; 2.00 mmol) and 4-(dimethylamino)pyridine (DMAP) (∼0.024 g; 0.1 mmol) were added. The solution was cooled in an ice bath to 0 °C, and 1,3-dicyclocarbodiimide (DCC) (0.413 g; 2.00 mmol) was added slowly to the reaction flask. The mixture was stirred in an ice bath for approximately 10 min before 2-iodoethanol (0.18 mL; 2.006 mmol) was added dropwise via syringe. This solution was stirred in an ice bath for ∼3 h and then was allowed to come to room temperature and stirring was continued overnight. The mixture was filtered, and the residue was washed with THF to dissolve any remaining product of the DCC coupling reaction. The solvent was removed in vacuo leaving a solid that was washed with cold chloroform (using gravity filtration). The chloroform dissolves the **PPIX-I** product and leaves the urea byproduct as a solid. The chloroform was removed under vacuum. The material was purified further using column chromatography (silica gel/CH_2Cl_2). The product was collected as a purple solid with a 50% yield after chromatography (some material sticks to the column) and was characterized by low- and high-resolution mass, UV−vis, and ^{1}H NMR spectroscopy and elemental analysis. LRMS−FAB *m*/*z*: 871 ($[M + 1]^+$), 745 ($[M - I]^+$), 635 ($[M - 2I + H_2O]^+$), 619 ($[M - 2I + 2H]^+$). HRMS−FAB: 870.11557, calcd 870.113910 $(M)^+$. UV−vis (CH_2Cl_2): 406 nm ($\epsilon = 1.65 \times 10^5$ M^{-1} cm^{-1}), 506 (1.50×10^4), 542 (1.25×10^4), 576 (7.53×10^3), 630 (5.86×10^3). ^{1}H NMR ($CDCl_3$, δ): −3.8 (s, 2H), 3.16 (t, $J = 6.8$, 4H), 3.31 (t, $J = 7.4$, 4H), 3.63 (s, 3H), 3.64 (s, 3H), 3.71 (s, 3H), 3.72 (s, 3H), 4.33 (t, $J = 7$, 4H), 4.42 (t, $J = 7.6$, 4H), 6.2 (d, $J = 11.6$, 2H), 6.38 (d, $J = 17.6$, 2H), 8.28 (dd, $J = 11.6$, 6, 2H), 10.04 (s, 1H), 10.08 (s, 1H), 10.17 (s, 1H), 10.22 (s, 1H). Anal. Calcd for $C_{38}H_{40}N_4O_4I_2$: C, 52.4; H, 4.60; N, 6.44. Found: C, 52.3; H, 4.49; N, 6.42.

[μ-S, μ-S′-Protoporphyrin IX Bis(2-thioethyl) diester]tetranitrosyldiiron (PPIX-RSE). A round-bottom flask equipped with a stir bar was charged with approximately 100 mL of distilled, deoxygenated THF. The solution was entrained with N_2, and the flask was then charged with Roussin's red salt, $Na_2[Fe_2(\mu\text{-}S)_2(NO)_4]\cdot 8H_2O$, (0.500 g; 1.03 mmol). The flask was sealed with a rubber septum, and the solution was kept under an inert atmosphere with a flow of nitrogen. A separate flask was charged with approximately 50 mL of distilled deoxygenated THF to which 0.897 g (1.03 mmol) of **PPIX-I** was added under dinitrogen. The RRS solution was then slowly transferred dropwise to this flask via a cannula with continuous stirring, and the resulting solution was allowed to stir overnight under an inert atmosphere. After this, the reaction mixture was filtered under N_2 and then evaporated under vacuum to dryness. The product was further purified via careful chromatography (silica gel/CH_2Cl_2/CH_3OH) to give a reddish-purple solid in 65% yield. This was characterized by low- and high-resolution mass, ^{1}H NMR, UV−vis, and IR spectroscopy and elemental analysis IR ($CHCl_3$): ν_{NO} bands at 1781 and 1754 cm^{-1}. LRMS−FAB *m*/*z*: 913 $(M + H)^+$, 822 $([M - 3NO]^+$. HRMS: found: 913.120488, 912.114887; theoretical: 913.118758 $(M + H)^+$, 912.110933 $(M)^+$. UV−vis (CH_2Cl_2): 406 nm ($\epsilon = 1.49 \times 10^5$ M^{-1} cm^{-1}), 506 (1.30×10^4), 538 (1.02×10^4), 576 (6.0×10^3), 632 (4.2×10^3). ^{1}H NMR ($CDCl_3$, δ): −3.8 (s, 2H), 1.1−1.9 (m, centered at 1.5, 8H closest to Fe), 3.38 (s, 3H), 3.48 (s, 3H), 3.66 (s, 3H), 3.7 (s, 3H), 3.8−4.9 (m, centered at 4.4, 8H closest to porphyrin ring), 6.21 (d, $J = 7.6$, 2H), 6.39 (d, $J = 14$, 2H), 8.28 (s, 2H), 10.1 (m, 4 H, porphyrin meso hydrogens).

Elemental analysis (C, H, N) for **PPIX-RSE** was performed by the Marine Science Analytical Laboratory at UCSB. Anal. Calcd for $C_{38}H_{40}N_8O_8Fe_2S_2$: C, 50.0; H, 4.39; N, 12.3; Fe, 12.3. Found: C, 49.8; H, 4.53; N, 10.2. The carbon and hydrogen values agree well with the expected values, but the nitrogen result is low. However, it should be noted that low N values are a common problem we have encountered in the analysis of such non-heme iron nitrosyl complexes, even though the values for other elements were very close to theoretical values. The iron content in the same sample was determined using a Shimadzu AA 6200 atomic absorption flame emission spectrophotometer with iron calibration curves generated with dried 99.9% Fe_2O_3 (Aldrich) digested in hot nitric acid and diluted in Nanopure water to appropriate concentrations (5−75 ppm). The Fe content was found to be 12.7 (±0.7)% (average of four individual samples), in very good agreement with the theoretical value.

Results and Discussion

Preparation and Properties of PPIX-RSE. The goals of the present study were to prepare a supramolecular compound combining the NO carrying function of Roussin's red salt Fe−S−NO cluster with an antenna **PPIX** chromophore having a strong absorption in the red and to study the photochemical properties of this material. The synthesis of **PPIX-RSE** from **PPIX** and Roussin's red salt is outlined in Scheme 1. A key step is the functionalization of **PPIX** to bis(2-iodoethyl) diester using a DCC coupling reaction. The reaction of the resulting **PPIX-I** with Roussin's red salt anion displaced both iodides to give **PPIX-RSE**, a relatively stable reddish-purple solid. Although X-ray quality crystals have not yet been obtained, the elemental analysis and high-resolution MS data have confirmed the molecular composition of **PPIX-RSE**, and the NMR, IR, and UV−vis spectra were fully consistent with the formulation represented to be the Roussin salt ester product of Scheme 1.

The electronic spectrum of **PPIX-RSE** is dominated by the porphyrin chromophore and is qualitatively and quantitatively very similar to that of **PPIX**. This is illustrated by Figure 1, which displays the spectra of both **PPIX-RSE** and **PPIX** in THF solutions. The lower section of Figure 1 displays the expanded visible-range spectra of **PPIX-RSE**, **PPIX**, and $Fe_2(SEt)_2(NO)_4$ (**I**) in THF and illustrates that the spectrum of **PPIX-RSE** is close to being the summed spectra of its two chromophores. In the IR spectra, the ν_{NO} bands of **PPIX-RSE** appear at nearly the same frequency as those seen for representative $Fe_2(SR)_2(NO)_4$ derivatives **I** (R = Et) and **II** ($R = CH_2Ph$). This is consistent with earlier studies[8] that showed NO stretching frequencies of Roussin's red salt esters to be relatively independent of the nature of the R− groups but markedly different from those of **RRS** or of monoalkylated RSE. Table 1 lists the peak maxima and extinction coefficients characterizing the optical spectrum of **PPIX-RSE** and the spectra of **I** and **II** and of **PPIX** itself. Also listed are the ν_{NO} frequencies for the iron cluster compounds.

Photochemical Studies. The quantitative photochemical reactions of Roussin's red salt anion and several red-salt esters, $Fe_2(NO)_4(SR)_2$, were previously studied[6,8,9] using changes in the electronic spectra to determine the quantum

(17) Gouterman, M.; Khalil, G. E. *J. Mol. Spectrosc.* **1974**, *53*, 88−100.

Scheme 1. Pathway for the Preparation of **PPIX-RSE**

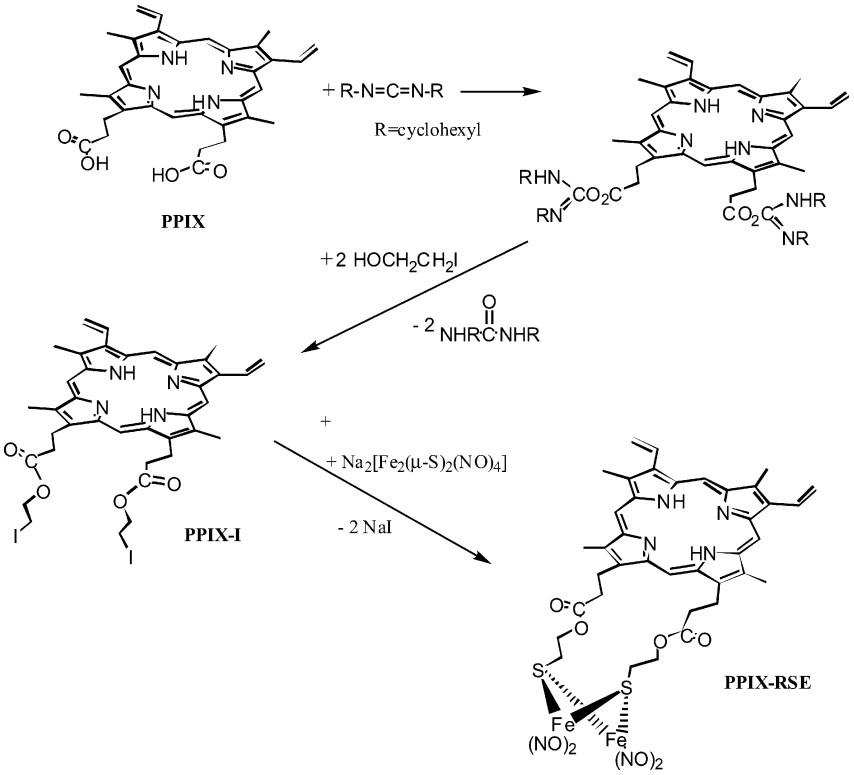

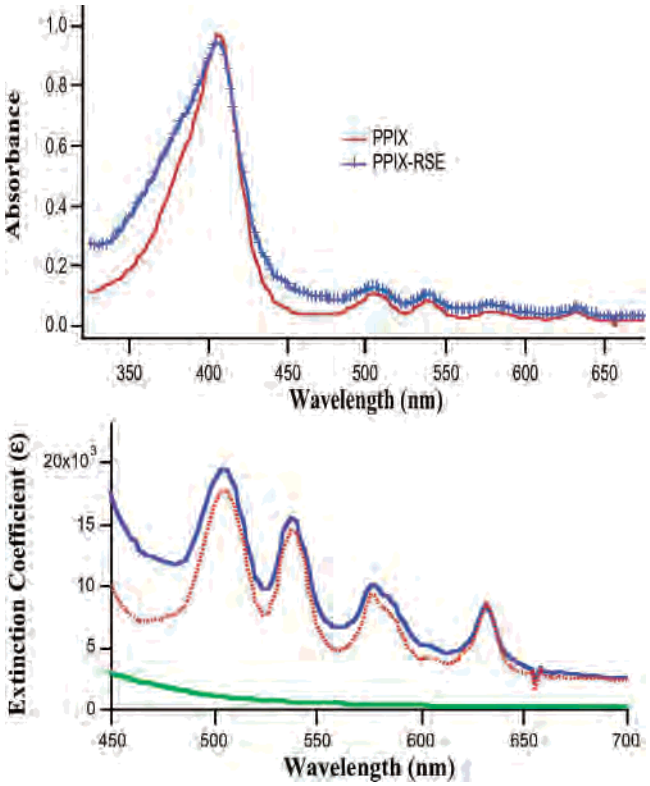

Figure 1. (Top) Electronic absorption spectra of **PPIX** (6.16 μM) and **PPIX-RSE** (6.02 μM) solutions in THF. Absorbances at the Soret band maximum are 0.89. These solutions were used for the steady-state emission measurements (Figure 3). (Bottom) Quantitative spectra of **PPIX-RSE** (blue), **PPIX** (red), and **I** (green) in THF in the Q-band region of the visible spectrum indicating that the spectrum of **PPIX-RSE** is close to being the summed spectra of its two chromophores.

yields for photodecomposition of these materials. When

Table 1. UV−Vis and IR Absorption Spectral Data for Various Ester Complexes in $CHCl_3$

compound	FTIR ν_{NO} (cm^{-1}) (log ϵ)	UV−vis λ_{max} (nm) (log ϵ)
$Fe_2(\mu\text{-}SCH_2CH_3)_2(NO)_4$ (**I**)	1750 (3.72) 1776 (3.77) 1800 (w)	310 (3.97), 364 (3.93) 430 sh (3.61)
$Fe_2(\mu\text{-}CH_2Ph)_2(NO)_4$ (**II**)	1751 (3.70) 1778 (3.74) 1800 (w)	312 (3.97), 364 (3.93)
PPIX		277 (5.49) 406 (Soret, 5.16) 504 (4.16), 538 (4.06) 576 (3.83), 632 (3.75)
PPIX-RSE	1754 (3.66) 1781 (3.70)	277 (5.56) 406 (Soret, 5.17) 506 (4.11), 542 (4.01) 576 (3.78), 630 (3.62)

coupled with the use of a nitric oxide-specific electrode, such optical spectral changes demonstrated that 0.5 NO was released per **RRS** anion decomposed,[6] whereas 4 NO was released by each **RSE**.[8] With **PPIX-RSE**, the photoreaction could not be conveniently monitored by changes in the optical spectrum because this was dominated by the porphyrin chromophore and underwent little change upon photolysis. Instead, these reactions were studied quantitatively by monitoring the changes in the IR spectra at frequencies characteristic of the ν_{NO} bands (Figure 2). Quantum yields (Φ_{dis}) determined in this way for the disappearance of these bands when **PPIX-RSE** and other representative **RSE** were photolyzed at the irradiation wavelengths (λ_{irr}) of 436 and 546 nm are listed in Table 2. For **I** and **II**, the Φ_{dis} values that were measured using IR detection were (within experimental uncertainty) the same as those determined by monitoring the optical absorbance

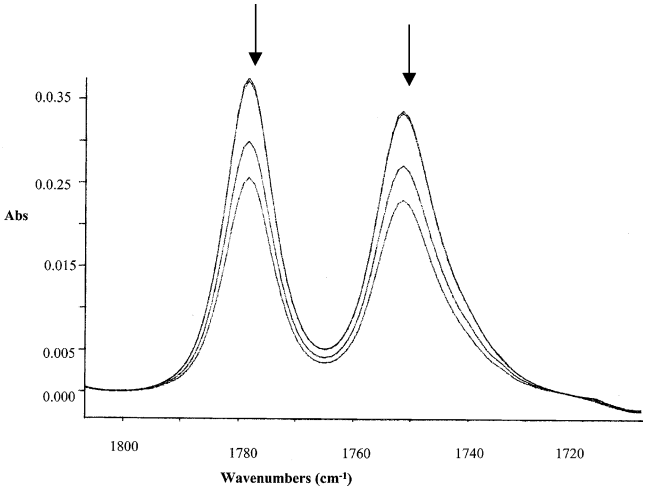

Figure 2. Absorbance changes of IR bands in the ν_{NO} spectral region upon 546-nm irradiation of $CHCl_3$ solutions of **PPIX-RSE**.

Table 2. Quantum Yields for the Decomposition of Various **RSE**s in $CHCl_3$ Solutions

compound	λ_{irr} (nm)	ϵ (λ_{irr})	Φ_{dis}[a] ($\times 10^4$)
$Fe_2(\mu\text{-}SCH_2Ph)_2(NO)_4]$ (**II**)	436	6.9×10^3	3.2 ± 0.1
	546	9.3×10^2	1.9 ± 0.3
$Fe_2(\mu\text{-}SEt)_2(NO)_4$ (**I**)	436	4.7×10^3	not determined
	546	7.6×10^2	1.7 ± 0.2
PPIX-RSE	436	3.2×10^4	5.2 ± 0.7
	546	1.2×10^4	2.5 ± 0.2

[a] The Φ_{dis} values represent quantum yields for the disappearance of the noted complexes from at least three independent measurements by monitoring absorbance changes of the IR nitrosyl stretching bands at 1780 and 1754 cm^{-1}. In each case, the concentrations were defined so that at λ_{irr} = 436 nm the intensity of absorbed light I_a was 3.0×10^{-6} Ein L^{-1} s^{-1} (I_o = 7.2×10^{-6} Ein L^{-1} s^{-1}). At 546 nm, $I_a = 1.0 \times 10^{-6}$ Ein L^{-1} s^{-1} ($I_o = 2.5 \times 10^{-6}$ Ein L^{-1} s^{-1}).

changes. Qualitative studies using a nitric oxide-specific electrode also demonstrated the concomitant photochemical-induced release of NO, and on the basis of earlier studies with other **RSE**s, it can be assumed that $\Phi_{NO} \approx 4\Phi_{dis}$.

As summarized in Table 2, Φ_{dis} is 2-fold larger at λ_{irr} = 436 nm than at 546 nm. (As shown before, photolysis at 365 nm gave considerably larger values of Φ_{dis} for other **RSE**s.)[8] Of special interest is the observation that the measured Φ_{dis} values for **PPIX-RSE** were ~50% higher at the respective λ_{irr} than those observed for both **I** and **II**. This is particularly significant because the porphyrin chromophore of **PPIX-RSE** dominates the optical spectrum of that compound and most of the incident light is absorbed by the porphyrin. **PPIX-RSE** displays photochemistry that is both qualitatively and quantitatively characteristic of the Fe/S/NO cluster core; therefore, initial excitation must be followed by nonradiative processes leading to the net reaction at the cluster core. In other words, there is no "inner filter" effect because of the unproductive absorption of light by the **PPIX** moiety; instead, the photochemical behavior is nearly the same as that seen by the direct excitation of closely related esters not having the pendant chromophore. Thus, there must be a high-efficiency energy transfer to the reactive state(s) because Φ_{dis} values are not diminished when the porphyrin serves as the primary chromophore. Because the porphyrin is the much stronger chromophore at longer wavelengths,

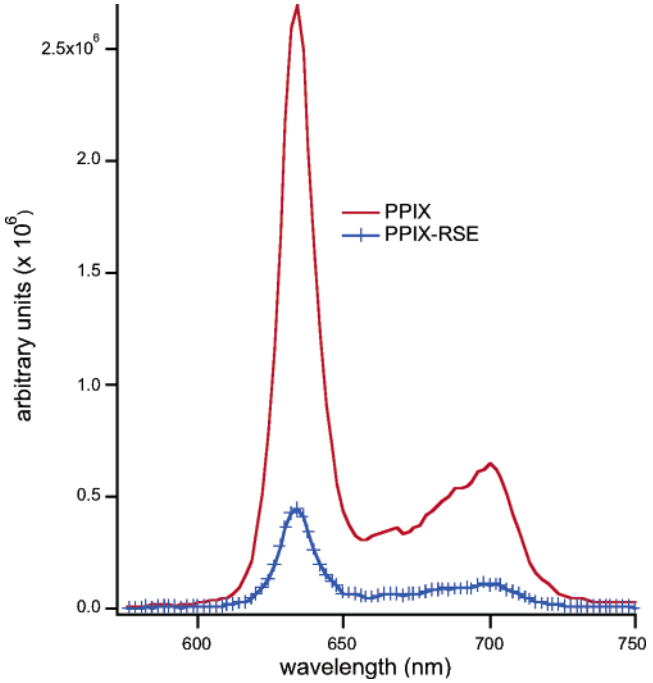

Figure 3. Fluorescence spectra of **PPIX** (6.16 μM) and **PPIX-RSE** (6.02 μM) in THF solutions with matched absorbances at the excitation wavelength (404 nm) under ambient conditions (22 ± 1 °C, aerated solutions).

PPIX-RSE is much more efficient at absorbing red light and converting it to the net photochemistry.

The greater photochemical efficiency of **PPIX-RSE** in the longer-wavelength photochemistry can be illustrated as follows. A 10 μM solution of $Fe_2(\mu\text{-}SEt)_2(NO)_4$ would have an absorbance (Abs) of 0.008 at an excitation wavelength of 546 nm (1-cm path length), whereas a 10 μM solution of **PPIX-RSE** would have an Abs of 0.12. The rate of NO photoproduction can be defined in terms of the intensity of the light absorbed, I_a, according to eq 2, where $I_a = I_o(1 - 10^{-Abs})$. Therefore, for a fixed incident light intensity I_o, the rate of NO photogeneration by **PPIX-RSE** at an initial concentration of 10 μM would be about 19-fold faster than for **I** at the same concentration.

$$\frac{\partial[NO]}{\partial t} = \Phi_{NO} I_a \qquad (2)$$

Emission Studies. The fluorescence spectra for **PPIX-RSE** and **PPIX** were recorded under ambient conditions in tetrahydrofuran solutions with concentrations (~6 μM) that gave matched absorbances (~1.0) at the 404-nm excitation wavelength. Figure 1 was generated from such a pair of solutions. Both solutions displayed fluorescence in the 630−740-nm range (largest peak at λ_{max} = 636 nm) characteristic of the porphyrin chromophore (Figure 3). However, the relative emission intensity from **PPIX-RSE** was only $^1/_6$ that from **PPIX**. Not surprisingly, red-salt esters **I** and **II** did not display any emission under comparable conditions. Equimolar (~6.8×10^{-6} M) solutions of $Fe_2(NO)_4(\mu\text{-}SEt)_2$ and **PPIX** together showed the same emission properties as the porphyrin alone; thus, there was little or no bimolecular quenching at these concentrations. Solutions of **PPIX** and

Table 3. TCSPC Fluorescence Lifetime Data for PPIX, **PPIX-DME**, and **PPIX-RSE** under Various Conditions (Ambient Temperature)

complex	solvent	τ (ns) ($\pm$ 0.5 ns) slower process	τ (ns) ($\pm$ 0.02 ns) faster process
PPIX-DME	$CHCl_3$	10.4	
PPIX-RSE	$CHCl_3$	8.6	0.23
mixture of PPIX-DME (2.5 μM) and **I** (4.2μM)	THF	12.6	
PPIX-DME	THF	12.6	
PPIX	THF	12.4	
PPIX-RSE	THF	10.7	0.22
PPIX-DME	THF (1 atm O_2)	5.4	
PPIX-RSE	THF (1 atm Ar)	14.6	0.20

PPIX-DME (the **PPIX** dimethyl ester) at equivalent concentrations displayed the same fluorescence intensity, so the reduced emission intensity from **PPIX-RSE** is not due to esterifying the **PPIX** carboxylic acid groups. Thus, the diminished porphyrin emission in **PPIX-RSE** must be specifically due to energy transfer from the pendant chromophore to the covalently linked iron−nitrosyl−sulfur cluster. Such intramolecular energy transfer must also explain the cluster photodecomposition resulting from direct excitation into the strongly absorbing porphyrin antenna.

The relative emission intensities from **PPIX-RSE** (I_f') and **PPIX** (I_f) can be used to estimate the lower limit for the rate constant of intramolecular quenching (k_q) according to the relationship $I_f/I_f' = 1 + k_q\tau$, where τ is the lifetime characteristic of **PPIX** (13 ns in ambient THF).[17] This would give $k_q = \sim 5 \times 10^8\ s^{-1}$. However, although such emission decreases have often been used to evaluate intramolecular quenching rates, the procedure is flawed by the assumption that intramolecular quenching is the only change in the **PPIX** photophysical properties upon linking this luminophore to the $Fe_2S_2(NO)_4$ cluster.

This assumption was tested by directly evaluating the emission lifetimes of **PPIX-RSE** and various **PPIX** derivatives using time-correlated single-photon counting (TCSPC) techniques. The excitation wavelength was 403 nm, and the absorbances at this λ_{irr} were 0.6 to 0.8. The temporal fluorescence behaviors of **PPIX**, **PPIX** dimethylester (**PPIX-DME**), and **PPIX-RSE** were measured under deaerated and aerated conditions in THF and $CHCl_3$ solutions. Although there were but modest differences in the emission lifetimes between ambient and deaerated solutions, the latter demonstrated longer-term stability. As will be noted below, the use of a pure O_2 atmosphere had a substantially larger effect on certain emission lifetimes. Selected data from the lifetime experiments are summarized in Table 3.

Fluorescence from **PPIX** (6.0 μM) in ambient THF demonstrated single-exponential decay curves from which the lifetime was determined to be 12.4 ns, in reasonable agreement with the reported value (13 ns, $\Phi \approx 0.1$).[17] The dimethyl ester **PPIX-DME** displayed a nearly identical lifetime (12.6 ns) in THF (4.46 μM) and a somewhat shorter one (10.4 ns) in $CHCl_3$ (4.26 μM). Thus, the lifetime results confirm the conclusion based on integrated emission intensities that esterification has little effect on the emission properties of the **PPIX** chromophore.

In marked contrast, the emission from **PPIX-RSE** was not a simple exponential but displayed two lifetime components,

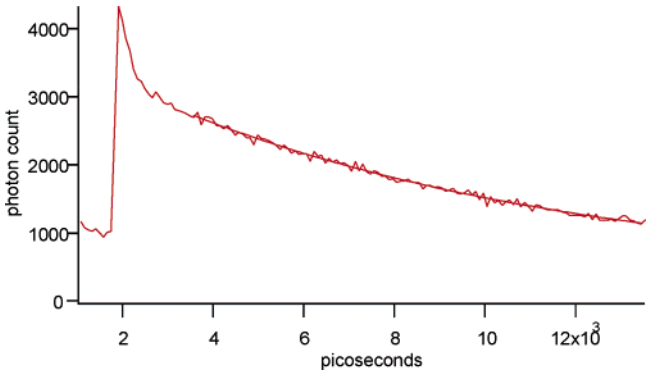

Figure 4. Fluorescence lifetime trace for **PPIX-RSE** (4.86 μM) in aerated THF showing dual emission behavior with $\tau_1 = 0.22$ ns and $\tau_2 = 10.7$ ns.

one quite short (~200 ps) and the other nearly as long as that of free **PPIX** (Figure 4). The dual lifetimes were obtained by good-quality fits of these decays to the biexponential function given by eq 3, where τ_1 and τ_2 are lifetimes, F_1 and F_2 are fractions of initial amplitude with a sum of 1.00, and A is a scaling factor. For **PPIX-RSE** in deaerated THF, this treatment gave $\tau_1 = 0.20 \pm 0.02$ ns ($F_1 = 0.82$) and $\tau_2 = 14.4 \pm 1$ ns ($F_2 = 0.18$). Exposing the solution to air had an insignificant effect on τ_1, but τ_2 decreased to ~11 ns. There appeared to be no time-dependent differences in the emission spectra, thus the porphyrin chromophore appears to be responsible for the emission under all circumstances.

$$I(t) = A[F_1 e^{-t/\tau_1} + F_2 e^{-t/\tau_2}] \quad (3)$$

A control sample consisting of **PPIX-DME** (2.51 μM) and $Fe_2(\mu\text{-}SCH_2CH_3)_2(NO)_4$ (4.2 μM) in argon-flushed THF displayed fluorescence that decayed exponentially, giving a single lifetime (12.6 ns) identical to that seen for **PPIX-DME** alone. Thus, consistent with the steady-state emission intensity experiments described above, there appears to be no bimolecular quenching of the **PPIX-DME** excited state by the RSE cluster at these concentrations. However, the emission lifetime of **PPIX-DME** (2.24 μM) in a THF solution equilibrated with O_2 at 1.0 atm was found to be only 5.4 ns, and bimolecular quenching by dioxygen would be appear to be playing a role. Under these conditions [O_2] $\approx$10 mM, so the quenching rate constant $k_q(O_2)$ can be roughly estimated to be $1 \times 10^{10}\ M^{-1}s^{-1}$, nearly diffusion-limited.

The dual emission seen for **PPIX-RSE** might be explained by the presence of two emitting species, the short-lived component being **PPIX-RSE** and the longer-lived one being a metal-free PPIX impurity. However, materials with identical temporal emission profiles and intensities were the result of several independent syntheses and repeated recrystallizations, so this is considered an unlikely explanation. Alternatively, progressive **PPIX-RSE** photodecomposition during the spectroscopic analytical procedures might release a more luminactive **PPIX** derivative from the iron cluster. Although enhanced emission from a longer-lived component was identified for an aerated THF solution of **PPIX-RSE** (4−8 μM) after continuous 365-nm photolysis, the dual emission property was also seen with fresh solutions. Nonetheless, to

minimize the release of a **PPIX** derivative during temporal fluorescence measurements, we restricted data collection to short periods with weak excitation beams and argon-flushed solutions, and we repeated lifetime determinations with fresh solutions. Such experiments gave excellent reproducibility of the dual lifetimes and amplitudes measured with τ_1 at 0.19−0.23 ns, τ_2 giving the value 14.4 ± 1 ns, and F_1/F_2 consistently in the 4.5−5 range. Furthermore, there was little change when the pump-laser intensity was increased by an order of magnitude. Thus, we conclude that the dual emission behavior is characteristic of the **PPIX-RSE** samples investigated.

The steady-state and flash-photolysis emission measurements are self-consistent. In the former, the emission intensity from **PPIX-RSE** was only about 17% of that seen for **PPIX** itself under nearly identical conditions. The temporal fluorescence behavior of analogous solutions of **PPIX** and **PPIX-DME** both display single-exponential decays with comparable relatively long lifetimes. In contrast, emission from the **PPIX-RSE** samples is bimodal; the largest component is much shorter lived than the smaller component, which has a lifetime comparable to that of **PPIX**. If one assumes that the radiative rate constant k_r for the porphyrin luminophore is the same in each case, then the relative fluorescence intensities under steady-state excitation are proportional to the relative lifetimes and the amplitude of their relative contribution ($I_i \propto F_i k_r \tau_i$). Accordingly, the short-lived component would contribute little to the integrated fluorescence spectrum of **PPIX-RSE**, and one would predict from the relative amplitudes of the two components that steady-state emission from **PPIX-RSE** would be diminished by at least 80% relative to that of **PPIX**. This is close to that what was seen given that modest changes in k_r values could impact this estimate.

The above data clearly indicate that the ∼80−85% reduction of the steady-state emission intensity and the dual-lifetime behavior relative to the simpler porphyrins are reproducible properties of **PPIX-RSE**. One explanation would be that the system is heterogeneous in the sense that this supramolecular species exists in two conformations, which interchange on a time scale longer than the fluorescence lifetime(s). Because the absorption spectrum of **PPIX-RSE** is dominated by the **PPIX** residue, both should have very similar absorption spectra, and the preexponential terms F_1 and F_2 would represent the fractions of the two species present. However, for the unlikely possibility that the absorption spectra of the two conformers differ significantly, this will not be true. Another possible explanation would be a sequential mechanism whereby all **PPIX-RSE** molecules have the same ground-state conformation, but after initial excitation, there is a very fast isomerization or reaction to give a second species with a lifetime comparable to that of free **PPIX**. This would almost have to be a conformational change or reversible bond cleavage given that (under Ar) there is little evidence for permanent chemical reactions under continuous photolysis conditions.

Summary

A porphyrin-derivatized Roussin red-salt ester, **PPIX-RSE**, was synthesized, characterized, and the photochemical and photophysical properties of this novel supramolecular compound were investigated. The quantum yield data revealed that **PPIX-RSE** is efficient at absorbing light and transferring energy from the excited porphyrin to the $Fe_2S_2(NO)_4$ cluster. The net result is the quenching of the porphyrin emission coupled to the photodecomposition of the cluster and concomitant NO dissociation. The emission studies support the concept that the porphyrin chromophore acts as a light-absorbing/transferring antenna molecule. The fluorescence intensity of **PPIX-RSE** is quenched by ∼85%, and the temporal fluorescence displays two components, the larger one with a lifetime of 0.20 ns and other with a τ of 14.4 ns in deaerated THF. The dual lifetime feature may be due to the presence of two ground-state conformers in solution with similar absorption spectra that, when excited, are too short lived to come to conformational equilibrium before undergoing decay.

Acknowledgment. These studies were supported by the National Science Foundation (CHE 9726889 and CHE 0095144). We are particularly indebted to Dr. James Bourassa, who provided guidance and inspiration at the initiation of this project.

IC049459A